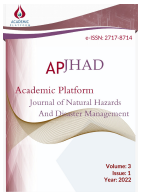

Research Article
Academic Platform Journal of Natural Hazards and Disaster Management
3(2), 72-84, 2022 DOI: 10.52114/apjhad.1201776

The Effect of Different Soil Classes on Earthquake Demands of Reinforced Concrete Structures: Case Study for Sakarya

Gökhan Dok[1*]

[1]Sakarya University of Applied Sciences (Earthquake Studies Research and Application Center, Turkey)

Received: / Accepted: 09-November-2022 / 27-December-2022

Abstract

In this study, it is aimed to investigate the effect of different soil classes on the behaviour of the structure under earthquake loads. An evaluation was made for five-storey and eight-story reinforced concrete (RC) frame structures considering the three different soil classes (ZC, ZD, ZE) defined in the Turkish Building Earthquake Code 2018 (TBEC 2018) and the current earthquake hazard of Sakarya. In the structural system of the RC frame, the cross-section geometry and reinforcement details of the columns and beams were designed by considering the design criteria in TBEC 2018. While determining the dynamic behaviour of the structure, the effective bending rigidity defined for column and beam elements in TBEC 2018 was used. For the RC frame structural model, the base shear force, story displacements and story drifts were investigated comparatively by using the mode superposition method in the SAP2000 finite element analysis program. When the results are compared, it is seen that as the soil stiffness decreases, the force and displacement demand on the structure increase.

Key words: Soil class, Turkish Building Earthquake Code 2018, Reinforced-concrete frame, Base shear, Structural demands

1. Introduction

Considering the current earthquake hazard in Turkey, structures are designed according to an important and non-negligible earthquake risk [1]. The design and evaluation of structures according to the current earthquake hazard are determined with the regulations defined in the Turkish Building Earthquake Regulation 2018 (TBEC 2018) [2]. Especially in the design of reinforced concrete (RC) structures, determining the earthquake loads predicted in TBEC 2018 and determining the earthquake demands on the structure are one of the most important steps for safety of structures [3]. Three different methods are used in the calculation of possible earthquake loads that structures may be exposed to, such as equivalent earthquake load, mode superposition method and time-history method [4]. The equivalent earthquake load method is suitable for regular and short buildings where high-mode effects are not significant [5]. The use of the mode superposition method and the time history method is more common in the design of structures as there is no regulation limiting the use of these two methods [6].

Mode superposition method is one of the most effective ways to determine the possible loads that will affect the structures and the dynamic behavior of the structures [4-7]. In this method, the possible earthquake acceleration that will affect the structure is determined by using the horizontal elastic acceleration spectrum defined in TBEC 2018 for each free vibration mode of

* Corresponding author e-mail: gokhandok@subu.edu.tr

the structures [5-8]. Each acceleration value obtained from the horizontal elastic acceleration spectrum in TBEC 2018, is converted into a base shear force by multiplying the modal mass corresponding free vibration mode [8, 9]. The base shear forces obtained for each vibration mode are combined with the square root method of the sum of the squares (SRSS) and the possible earthquake force that may affect the structure is calculated [7-10]. Apart from this mathematical combination method, the complete quadratic combination (CQC) method can also be used [10, 11]. The dynamic behavior of the structure is analyzed under these earthquake loads [9-12]. The base shear force values obtained for each free vibration mode are applied to the story levels in accordance with the mode shapes of the structure [3, 8, 13]. As a result of the analysis, storey displacements and drifts, deformation and internal force distribution of the structural elements are examined [7, 14, 15].

In the mode superposition method, all analysis results such as storey displacements and relative storey drifts, normal force, moment and shear force on structural elements are combined mathematically with SRSS or CQC [3, 7, 16]. Structural elements are designed according to superposed displacements and internal forces, and structural safety is ensured against predicted earthquake loads [1, 3, 7]. Control of section geometry and reinforcement details in RC elements are calculated according to superposed earthquake demands [4-7]. For this reason, it is of great importance to determine the earthquake loads according to the existing earthquake hazard in RC structures [14-16]. Additionally, it is foreseen that the displacement demands depending on the soil may change, especially considering the soft soil conditions [17,18]. In the literature, it has been concluded that the spectral accelerations obtained from the earthquake hazard map in TBEC 2018 greatly increase the spectral accelerations in weak-strength soils and in cases where the period of the structure is less than 1s [19, 20]. Moreover, the spectral accelerations obtained according to the current earthquake hazard in TBEC 2018 increased by a minimum of 50% and in some regions more than 100% in the spectral accelerations obtained according to the predicted earthquake hazard in 2007 [21-23]. For this reason, it is of great importance to correctly calculate the earthquake demands due to the existing earthquake hazard in critical regions such as Sakarya with building height limitations, soft soil profile and soil liquefaction potential [24-26].

In the study, six mode superposition method were performed by using SAP2000 finite element software [27] for three-dimension, five-storey and eight-storey RC structures on different soil classes. The force and displacement demand on the structure were determined according to the dynamic behaviour of the structure and the horizontal elastic acceleration spectrum in TBEC 2018. According to the result of spectrum analysis, the variation of the structural demands (force and displacement) were examined considering the total height of the structure and the effect of soil classes in TBEC 2018.

Considering the earthquake risks in TBEC 2018, it has been observed that the studies conducted for regions with very low shear wave velocity such as Sakarya for different earthquake levels are generally on two-dimensional structures. This study shows the change of the earthquake forces based on the design for the structures to be built in cities with a soft soil profile such as Sakarya. In addition to, the increase in the number of story and the softening of the soil indicate that the increase in the ductility demand in the structures increases proportionally. It also reveals that the control of the story drifts obtained from the analysis is very important even if the design is made in accordance with the rules in the regulations. Therefore, it is an important case study that presents important data to designers and contributes in the literature.

2. Materials and Methodology

The three-dimensional view of structural SAP 2000 model is shown in Figure 1. The section geometry and reinforcing details of the RC structure were designed in accordance with the regulations of TBEC 2018 and Requirements for design and construction of reinforced concrete structures (TS 500-200) [2, 28].

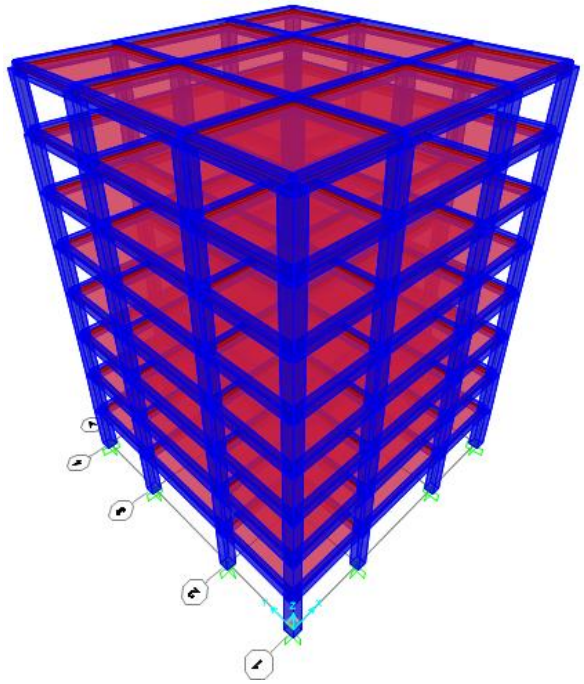

Figure 1. The 3D view of SAP 2000 model

The material, section geometry and reinforcing details of structural elements (column and beams) are given in Table 1. In the structures analysed in the study, all column sections were considered the same on all stories in order to prevent stiffness irregularities (soft story) between stories.

Table 1. The material, section geometry and reinforcing details of structural elements

Section	Conc.-Reinfor. Class	Elasticity Modulus of Conc.-Reinfor. (Mpa)	Dimensions (mm)	Long. Reinfor. (mm)	Trans. Reinfor. (mm)
Columns	C30-S420	30000-210000	600x600	12Φ20	Φ10/80
Beams	C30-S420	30000-210000	400x600	8Φ16	Φ10/100

The shear strength of the structural members was calculated according to TBEC 2018 and it was seen that the structural members had sufficient shear strength against possible design shear forces. The moment capacity was determined considering moment-curvature relationships of beams and columns and are shown in Figure 2 [29]. For the structural models examined in this study, the axial loads obtained under earthquake loads vary between 50 and 2400 kN. Moment curvature analyses were compared under the maximum axial loads obtained for the columns and it was seen that the moment capacity did not change to a large extent. For this reason, the average axial load value under earthquake loads was used and the average constant axial load value on the columns was accepted as 1200 kN. The value of 0.11 is obtained by dividing the design axial load (N_d) by the product of the characteristic concrete strength and the cross-sectional area ($f_{ck}*A_c$).

The moment-curvature relationships were calculated by using a step by step solution under a constant axial load value for columns [30, 31]. Similarly, the moment-curvature relationships of beams were examined without any axial load in sectional analysis. The limit strain values and corresponding yield and ultimate strengths of reinforcements, confined and unconfined concrete were used to determine moment-curvature relationships of all RC sections considering Mander confined and unconfined concrete model [32]. The moment-curvature analysis was performed by using the step-by-step incremental analysis method considering concrete and reinforcement deformations. Additionally, the moment-curvature relationship was obtained by step-by-step analysis of the force balance consisting of tensile and compressive forces in the section considering Mander confined and unconfined concrete models. In these analyses, the moment is obtained at every step by using the lever arm formed between the compressive force depending on the deformation in concrete and the tensile force resulting from elongation deformations in tensile reinforcement. Curvature is the unit rotation angle of a cross-section corresponding flexural moment value and is calculated by using the derivative of the inclination of the tangent with respect to arc length in the unit deformation diagram. The moment-curvature relationship was given to show graphically effective bending rigidity, ductile design, and maximum flexural capacity of RC structural elements obtained according to the TBEC 2018.

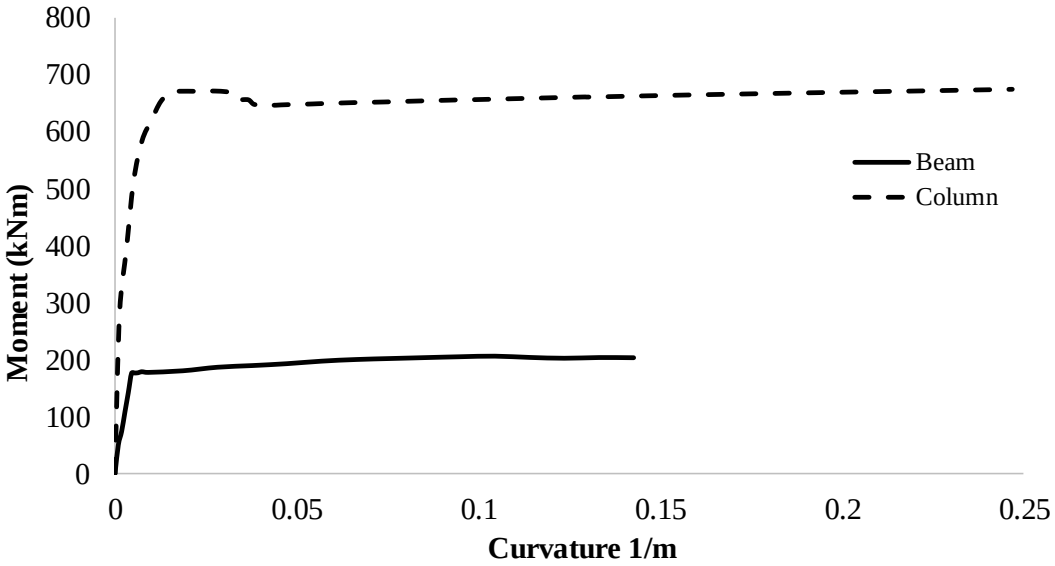

Figure 2. The moment-curvature relationships of beams and columns

The plan view and the general layout of three dimensional structural SAP2000 model are shown in Figure 3. While the dead and live loads on slabs are assumed as 2 kN/m^2, only the live loads on roof story are selected as 1.5 kN/m^2. The effective bending rigidity ($EI_{effective}$) of beams and columns are identified as 0.35 and 0.7 times initial stiffness (EI) considering the values defined in TBEC 2018. The weights of structures are calculated by taking into account the necessary regulations for residential buildings in TBEC 2018, with the sum of dead loads and live loads 0.3 times (G+0.3Q).

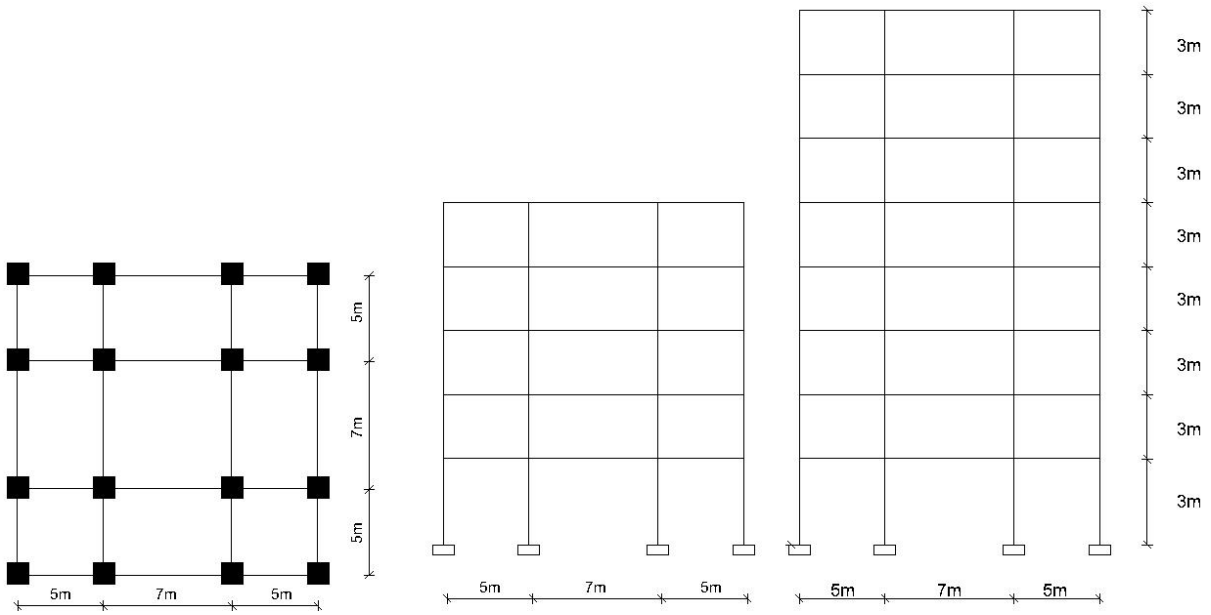

Figure 3. The plan view, the general layout and 3D view of structural SAP 2000 models

In the study, the mode superposition method was performed to determine structural demands considering current earthquake risk of Sakarya defined in TBEC 2018 [2, 33]. The earthquake hazard map of Disaster and Emergency Management Presidency (AFAD) was used to define the horizontal elastic acceleration spectrum (Fig. 4). The horizontal elastic acceleration spectrum was determined for the design earthquake, that is, the DD-2 earthquake level, with a 10% probability of exceedance in 50 years and a reoccurrence period of 475 years [33]. These spectrums for each different soil class (ZC, ZD, ZE) were composed for a residential-type RC structure located at latitude 40.779 and longitude 30.357 in Serdivan district of Sakarya province. Soil classes ZA and ZB defined in TBEC 2018 are defined as very hard rock or bedrock. In this study, soft soil conditions common in Sakarya region were investigated.

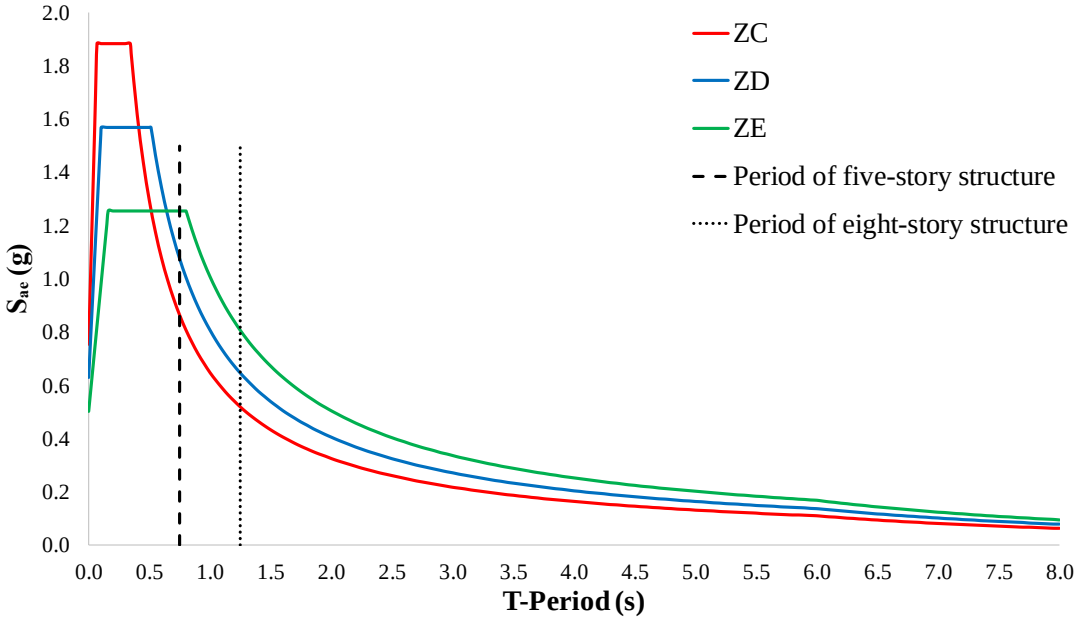

Figure 4. The horizontal elastic acceleration spectrum for different soil classes

The horizontal elastic acceleration spectrum was determined considering the equations Eqs. 1-6 defined in TBEC 2018.

$$S_{ae}(T) = \left(0.4 + 0.6\frac{T}{T_A}\right) \qquad (0 \le T \le T_A) \qquad (1)$$

$$S_{ae}(T) = S_{DS} \qquad (T_B \le T \le T_A) \qquad (2)$$

$$S_{ae}(T) = \frac{S_{D1}}{T} \qquad (T_B \le T \le T_A) \qquad (3)$$

$$S_{ae}(T) = \frac{S_{D1} * T_L}{T^2} \qquad (T_B \le T) \qquad (4)$$

$$S_{DS} = S_S * F_S \qquad (5)$$

$$S_{D1} = S_1 * F_1 \qquad (6)$$

In these formulations, the free vibration period of the structure, corner periods of the spectrum curve, and elastic spectral acceleration are represented by T, T_A, T_B, and $S_{ae}(T)$, respectively. The corner periods are calculated by using Eqs. 7 and 8.

$$T_A = 0.2\,\frac{S_{D1}}{S_{DS}} \qquad (7)$$

$$T_B = \frac{S_{D1}}{S_{DS}} \qquad (8)$$

The S_S and S_1 are used as map spectral acceleration coefficients. Additionally, the S_{DS} and S_{D1} are selected design spectral acceleration coefficients. Furthermore, F_S and F_1 are determined as local soil class coefficient for short period region and for 1.0 second period region, respectively. All coefficients are calculated by using AFAD earthquake hazard map and TBEC 2018 regulation defined in Table 2 and 3. The soil classes defined in TBEC 2018 and used in this study are categorized in Table 4. The classification characteristics of soil classes are explained in detail according to the soil types. In TBEC 2018, especially the 1 second period was accepted as the critical threshold. For this reason, the spectral acceleration coefficient SD1 corresponding to 1 second period is calculated together with SDS. The structures analysed in this study were designed with periods greater than and less than 1 second.

Table 2. Local soil class coefficients for the short period region

Soil class	Local ground effect coefficient for short period region F_S					
	$S_S \le 0.25$	$S_S = 0.50$	$S_S = 0.75$	$S_S = 1.00$	$S_S = 1.25$	$S_S \ge 1.50$
ZA	0.8	0.8	0.8	0.8	0.8	0.8
ZB	0.9	0.9	0.9	0.9	0.9	0.9
ZC	1.3	1.3	1.2	1.2	1.2	1.2
ZD	1.6	1.4	1.2	1.1	1.0	1.0
ZE	2.4	1.7	1.3	1.1	0.9	0.8
ZF	Site-specific soil behavior analysis will be carried out					

Table 3. Local soil class coefficients for 1.0 second period region

Soil class	Local ground effect coefficient for 1.0 second period region F_1					
	$S_1 \le 0.10$	$S_1 = 0.20$	$S_1 = 0.30$	$S_1 = 0.40$	$S_1 = 0.50$	$S_1 \ge 0.6$
ZA	0.8	0.8	0.8	0.8	0.8	0.8
ZB	0.9	0.9	0.9	0.9	0.9	0.9
ZC	1.3	1.3	1.2	1.2	1.2	1.2
ZD	1.6	1.4	1.2	1.1	1.0	1.0
ZE	2.4	1.7	1.3	1.1	0.9	0.8
ZF	Site-specific soil behavior analysis will be carried out					

In the mod superposition method, the sufficient number of modes are calculated considering %95 participating ratio of modal mass or above. Three dimensional (3D) structural SAP 2000 model of five-story and eight-story RC-frame structures were analysed by using the mode superposition method. In the mode superposition method, all analysis results such as story displacements and relative story drifts, normal force, moment and shear force on structural elements are combined mathematically with SRSS or CQC. Structural elements are designed according to superposed displacements and internal forces, and structural safety is ensured against predicted earthquake loads.

Table 4. Soil classes

Soil class	Soil type	Top 30 meters average		
		$(V_s)_{30}$ (m/s)	$(N_{60})_{30}$ (impact/30 cm)	$(c_u)_{30}$ (kPa)
ZA	Solid, hard rocks	>1500	-	-
ZB	Less weathered, moderately strong rocks	760-1500	-	-
ZC	Very tight layers of sand, gravel and hard clay or weathered, highly fractured weak rocks	360-760	>50	>250
ZD	Medium firm – firm sand, gravel or very solid clay layers	180-360	15-50	70-250
ZE	Loose sand, gravel or soft-solid clay layers or profiles with PI > 20 and w > 40%, containing a total layer of soft clay (cu < 25 kPa) thicker than 3 meters in total	<180	<15	<70
ZF	Site-specific soil behaviour analysis will be carried out			

Besides, the distribution of the base shear force to the stories was performed in accordance with each free vibration mode. The lateral earthquake load calculated according to horizontal acceleration spectrum of TBEC 2018 were carried out in both directions of structures. However, since the structure is architecturally and statically symmetrical in the x and y directions, only the results in the x direction were evaluated. The results were examined by comparing base shear forces, roof and story displacements, relative story drifts considering the effect of horizontal acceleration spectrum of TBEC 2018 for different soil classes (ZC, ZD, ZE). This comparison was examined for five and eight-storey RC structures, and the effect of the number of stories on the results was obtained.

3. Results and Discussions

The structural demands are determined considering the dynamic behaviour of five and eight – storey SAP2000 models. The dynamic characteristics such as periods, frequency and modal parameters are given Table 5 in detail.

The sufficient number of modes for five and eight-storey structural models are obtained as 11 and 12, respectively. The total mass participation ratios in these modes were calculated as 99.2% in the translation in the x and y directions and 96.8% in the rotation (torsion) axis around the z vertical axis for the five-storey structure. Additionally, the same ratios were obtained as 96.8% in all axes of freedom for the eight-storey structure.

The superposed base shear forces and roof displacements obtained from the TBEC 2018 elastic horizontal acceleration spectrum according to soil classes are given in Table 6.

Table 5. The dynamic characteristics and modal parameters

	Mode	Period (s)	Frequency (Hz.)	Modal participating mass ratio (%)					
				UX	UY	SumUX	SumUY	RZ	SumRZ
Five-storey model	1	0.750	1.333	72.9	7.6	72.9	7.6	0.0	0.0
	2	0.750	1.333	7.6	72.9	80.5	80.5	0.0	0.0
	3	0.657	1.521	0.0	0.0	80.5	80.5	80.5	80.5
	4	0.226	4.433	6.2	5.3	86.7	85.7	0.0	80.5
	5	0.226	4.433	5.3	6.2	91.9	91.9	0.0	80.5
	6	0.198	5.047	0.0	0.0	91.9	91.9	11.4	91.9
	7	0.116	8.628	4.6	0.2	96.6	92.1	0.0	91.9
	8	0.116	8.628	0.2	4.6	96.8	96.8	0.0	91.9
	9	0.102	9.813	0.0	0.0	96.8	96.8	4.9	96.8
	10	0.073	13.739	0.2	2.2	97.0	99.0	0.0	96.8
	11	0.073	13.739	2.2	0.2	99.2	99.2	0.0	96.8
	Mode	Period (s)	Frequency (Hz.)	Modal participating mass ratio (%)					
				UX	UY	SumUX	SumUY	RZ	SumRZ
Eight-storey model	1	1.246	0.803	0. 3	79.5	0.3	79.5	0.0	0.0
	2	1.245	0.803	79.5	0.3	79.8	79.8	0.0	0.0
	3	1.089	0.918	0.0	0.0	79.8	79.8	79.9	79.9
	4	0.392	2.550	0.0	10.4	79.8	90.2	0.0	79.9
	5	0.392	2.552	10.4	0.0	90.2	90.2	0.0	79.9
	6	0.344	2.909	0.0	0.0	90.2	90.2	10.2	90.1
	7	0.213	4.688	0.0	04.2	90.2	94.4	0.0	90.1
	8	0.213	4.695	4.2	0.0	94.4	94.4	0.0	90.1
	9	0.188	5.325	0.0	0.0	94.4	94.4	4.2	94.4
	10	0.137	7.300	0.0	2.4	94.4	96.8	0.0	94.4
	11	0.137	7.318	2.4	0.0	96.8	96.8	0.0	94.4
	12	0.121	8.289	0.0	0.0	96.8	96.8	2.4	96.8

When the Table 4 and Table 6 were examined, it was observed that the base shear force on the structure increased as the shear wave velocity on the soil decreased for both structural models. Similarly, it is seen that the displacement demand of the structure increases as the soil stiffness decreases and the soil softens when the analysis results are examined. When the ZC soil is taken as reference, the base shear force increased up to 43% for 5-storey structures and up to 53% for 8-storey structures. Besides, the roof displacement of the structure increased up to 50% for 5-storey structures and up to 70% for 8-storey structures. Additionally, as the number of stories increases, it has been determined that there may be an increase of 50-70% in the roof displacement depending on the soil class.

Table 6. The superposed baser shear forces according to the soil classes

Soil class	Base shear force (kN)		Roof displacements (m)	
	Five-storey structure	Eight-storey structure	Five-storey structure	Eight-storey structure
ZC	1518.8	1428.2	0.020	0.030
ZD	1859.4	1805.1	0.025	0.041
ZE	2174.6	2181.2	0.030	0.051

The variation of story displacements according to the soil class and the number of stories are shown in Figure 5 for five and eight-story structures, respectively. On the other hand, it has been observed that the change in the base shear force according to the number of stories in the structure can be obtained between 0.3-6% as both an increase and a decrease.

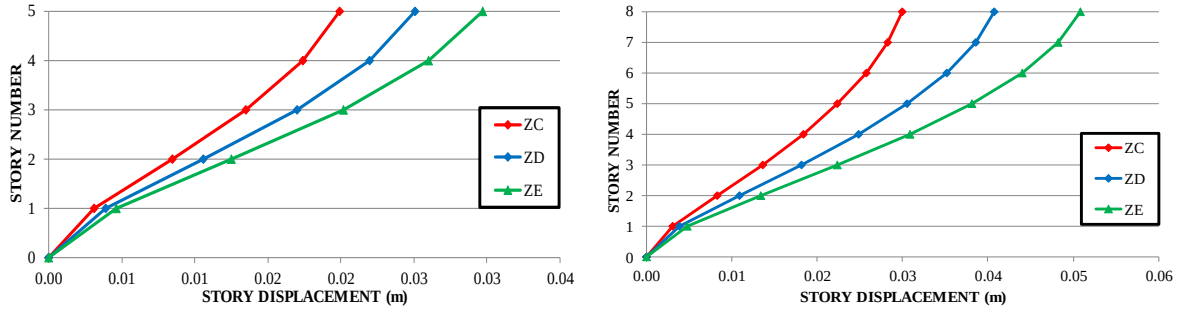

Figure 5. The storey displacements a) for five-storey b) eight-storey structural model

It has been seen that the storey displacements increased as the stiffness of soils decreased just as the roof displacements. It should be noted that the difference between the story displacements of structures built on different soil classes increased as the number of stories increased.

In this study, the story drifts are calculated by using the equations Eqs. 9-11 defined in TBEC 2018.

$$\Delta_i^{(X)} = u_i^{(x)} - u_{i+1}^{(x)} \tag{9}$$

$$\delta_i^{(X)} = \frac{R}{I} * \Delta_i^{(x)} \tag{10}$$

$$\lambda \frac{\delta_{i,max}^{(X)}}{h_i} \leq 0.008\,\kappa \tag{11}$$

In these equations, the difference of storey displacements between top and bottom stories and the story height are represented as $\Delta_i^{(X)}$ and h_i. The R and I are identified in TBEC 2018 as structural system behaviour coefficient and building importance coefficient and are obtained from TBEC as 8 and 1, respectively. The K is a coefficient accepted as 1 for RC structures. The λ is calculated by dividing the spectral acceleration corresponding to the structure period in the horizontal elastic acceleration spectrum for DD-3 earthquake risk by the spectral acceleration corresponding to the structure period in the horizontal elastic acceleration spectrum for DD-2 earthquake risk in TBEC 2018. The variation story drifts are shown in Figure 6. The limit value calculated for story drifts was obtained as 0.008 by applying the equations 9-11 defined in TBEC 2018.

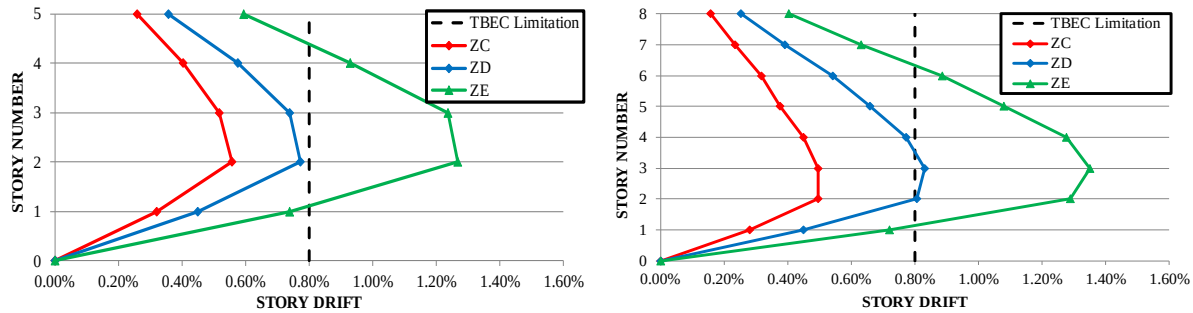

Figure 6. The storey drifts a) for five-storey b) eight-storey structural model

When the Table 4 and Figure 6 were examined together, it was seen that the story drifts were found to be inversely proportional to the shear wave velocity on the soils for both structural models. However, this relationship does not show a linear increase or decrease. Additionally,

as the number of stories increased, the story drifts reached greater values and it was observed that the highest value occurred in the ZE soil class. Besides, the story drifts obtained for ZE in 5 and 8 storey structural models exceeded the limit values in TBEC 2018 and reached levels that would endanger the safety of the structure under earthquake loads. The story drift calculated for the ZC in the five-storey model showed an increase of 30% for ZD and 217% for ZE. Similarly, the story drift obtained for the ZC in the eight-storey structure increased by 60% for ZD and 280% for ZE. When all the results are examined, it can be said that the story drifts increase as the soil stiffness and shear wave velocity in the soil decrease. The most unfavourable situation was obtained for the ZE soil class and the eight-story structure.

4. Conclusions

In this numerical study, six mode superposition method were carried out for three-dimension, five-storey and eight-storey RC structures on different soil classes. The variation of story drifts, force and displacement demands due to earthquake loads were evaluated by using the horizontal elastic acceleration spectrum in TBEC 2018 and modal response of the structures. The structural demands were determined considering the sufficient number of mods that provide a mass participation ratio of 95% and above. The results of mode superposition analysis were compared considering the total height of the structure and the effect of soil classes in TBEC 2018. According to the analysis results, the following conclusions can be concluded:

1) When the maximum base shear forces are compared, the base shear force on the structure increased as the shear wave velocity and the stiffness of the soils decreased. The base shear force increased up to 43% for 5-storey structures and up to 53% for 8-storey structures compared with the base shear forces of the structures on ZC soil. The largest base shear forces were obtained in the analysis of ZE soil for both structural models.

2) It has been observed that the roof displacement of the structure is inversely proportional to the shear wave velocity on the soils for both structural models. However, this proportional relationship does not show a linear increase or decrease. As the soil soften, the roof displacement of the structure increased up to 50% and up to 70% for 5-storey and 8-storey structures, respectively. It should be noted that there is a negative effect of number of stories on the roof displacement and story displacements. It has been observed that as the number of stories in the structure increases, the total displacement demand of the structure reaches greater values.

3) It has been seen that the story drifts increased with the decreasing soil stiffness and shear wave velocity for all structural models. Additionally, the most unfavourable values were obtained for the softest soils (ZE) for both five and eight-storey structures. Furthermore, the story drift values of ZE in both structures exceeded the limitations of TBEC 2018. The increase of story drifts is obtained as 30-60% for ZD and 217-280% for ZE. When all the results are examined, the story drifts increase as the soil stiffness and shear wave velocity in the soil decrease. On the other hand, it has been observed that the number of stories is less effective for the story drifts when compared to the effect of soil class.

In this study, it is concluded that the structural performance of five and eight-storey structural RC FEM models are determined considering dynamic behaviour of structure and horizontal acceleration spectrum of TBEC by using mode superposition method. It should be noted that more numerical analysis using different structural models is necessary to obtain more general results.

Conflict of Interest

The authors declare that they have no known competing financial interests or personal relationships that could have appeared to influence the work reported in this paper.

Author Contribution

G. Dok designed the structural finite element model and the computational framework, and carried out the calculations considering the implementation and wrote the manuscript.

References

[1] Z. Celep, Deprem Mühendisliğine Giriş ve Depreme Dayanıklı Yapım Tasarımı. Istanbul: Birsen Yayınevi, 2019.

[2] The Ministry of Environment, Urban and Climate Change. "Turkish Building Earthquake Code, TBEC 2018." Turkey, 2018.

[3] K. Darılmaz, Depreme Dayanıklı Binaların Tasarımına Giriş. Istanbul: Birsen Yayınevi, 2019.

[4] T., Uçar, O. Merter. (2012, Dec.) "Binaların deprem hesabında kullanılan doğrusal elastik hesap yöntemleriyle ilgili bir irdeleme." *Ordu Üniversitesi Bilim ve Teknoloji Dergisi.* 2 (2), pp. 15–31. Available: https://dergipark.org.tr/tr/download/article-file/113887

[5] V., Başaran, M. Hiçyılmaz. (2020, June) "Betonarme çerçevelerde farklı deprem yer hareketi düzeyi etkilerinin incelenmesi." *Journal of Innovations in Civil Engineering and Technology.* 2 (1), pp. 27–41. Available: https://dergipark.org.tr/tr/download/article-file/1176258

[6] M. Fragiadakis. (2013, Jan.) "Response spectrum analysis of structures subjected to seismic actions." *Encyclopedia of Earthquake Engineering.* pp. 3–18. Available: https://link.springer.com/referenceworkentry/10.1007/978-3-642-36197-5_133-1

[7] A. Doğangün, Deprem-Zemin ve Depreme Dayanıklı Yapı Tasarımı. Istanbul: Birsen Yayınevi, 2021.

[8] E. Canbay, U. Ersoy, G., Özcebe, H. Sucuoğlu, T. S. Wasti, Binalar için Deprem Mühendisliği Temel İlkeler. Istanbul: Bizim Büro Basımevi, 2008.

[9] M.N., Aydinoglu. (2003, Jan.). "An Incremental Response Spectrum Analysis Procedure Based on Inelastic Spectral Displacements for Multi-Mode Seismic Performance Evaluation." *Bulletin of Earthquake Engineering.* (1), pp. 3–36. Available: https://link.springer.com/article/10.1023/A:1024853326383

[10] A.K. Chopra, R.K. Goel, Modal pushover analysis of sac buildings. California: PEER, 2001.

[11] A.K., Chopra, R.K., Goel. (2002, Dec.). "A Modal Pushover Analysis Procedure for Estimating Seismic Demands for Buildings." *Earthquake Engineering Structural. Dynamics.* (31), pp. 561–582. Available: https://onlinelibrary.wiley.com/doi/10.1002/eqe.144

[12] M.J.N. Priestley. "Performance Based Seismic Design", 12th World Conference on Earthquake Engineering, 2000, pp. 325–346.

[13] P, Fajfar. (2000, Dec.). "A Nonlinear Analysis Method for Performance-Based Seismic Design." *Earthquake Spectra,* 16 (3), pp. 573–592, Available: https://journals.sagepub.com/doi/10.1193/1.1586128

[14] P. Fajfar. "Structural analysis in earthquake engineering – A breakthrough of simplified non-linear methods", Proceedings of 12th European Conference on Earthquake Engineering, 2002, Paper No. 843.

[15] Peter J. Stafford, Julian J. Bommer. "Ground motions for performance-based earthquake engineering" Theoretical Consistency of Common Record Selection Strategies in Performance-Based Earthquake Engineering, 1, 13, M.N. Fardis, Ed Springer Dordrecht Berlin: Springer Science+Business Media B.V., 2010 pp. 3-14,

[16] H. Duan and M.B.D. Hueste (2012). "Seismic performance of a reinforced concrete frame building in China." *Engineering Structures.* (41), pp. 77-89. Available: https://www.sciencedirect.com/science/article/pii/S0141029612001484

[17] E.L. Wilson, A. Der Kiureghian, E.P., Bayo (1981, Apr.). "A replacement for the SRSS method in seismic analysis." *Earthquake Engineering and Structural Dynamics. 9* (2), pp. 187–192. Available: https://doi.org/10.1002/eqe.4290090207

[18] A. Der Kiureghian, (1981, Apr.). "A response spectrum method for random vibration analysis of MDF systems." *Earthquake Engineering and Structural Dynamics. 9*, pp. 187–192. Available: https://doi.org/10.1002/eqe.4290090503

[19] A. J. Salmonte. (1982, Apr.) "Consideration on the residual contribution in modal analysis." *Earthquake Engineering and Structural Dynamics.* 10 (2), pp. 295–304. Available: https://doi.org/10.1002/eqe.4290100210

[20] V. Başaran. (2018, Dec.). "Türkiye Bina Deprem Yönetmeliğine (TBDY2019) göre Afyonkarahisar için deprem yüklerinin değerlendirilmesi." *Afyon Kocatepe Üniversitesi Fen ve Mühendislik Bilimleri Dergisi.* 18, pp. 1028-1035. Available: https://dergipark.org.tr/tr/pub/akufemubid/issue/44157/544663

[21] Ö. Çavdar, A. Yolcu. (2018, Dec.). "Mevcut bir okul binasının Türk Bina Deprem Yönetmeliği 2018'e göre yapısal düzensizliklerinin incelenmesi." *Ordu Üniversitesi Bilim ve Teknoloji Dergisi. 8* (2), pp.153–164. Available: https://dergipark.org.tr/tr/download/article-file/619059

[22] T. Kap, E. Özgan, M.M., Uzunoğlu. (2019, July). "Betonarme bir okul binasının 2018 Deprem Yönetmeliğine göre incelenmesi." *Düzce Üniversitesi Bilim ve Teknoloji Dergisi.* 7 (3), pp. 1140–1150. Available: https://dergipark.org.tr/tr/download/article-file/619059

[23] E. Keskin, K.B., Bozdoğan. (2018, June). "2007 ve 2018 Deprem Yönetmeliklerinin Kırklareli İli özelinde değerlendirilmesi." *Kırklareli University Journal of Engineering and Science.* 4 (1), pp. 74–90. Available: https://dergipark.org.tr/tr/download/article-file/619059

[24] M., Öztürk. (2018, Sep.). "Türkiye Bina Deprem Yönetmeliği ve Türkiye deprem tehlike haritası ile ilgili İç Anadolu Bölgesi bazında bir değerlendirme." *Selçuk Teknik Dergisi.* 17 (2), pp. 31-42. Available: https://dergipark.org.tr/tr/download/article-file/619059

[25] E., Seyrek. (2020, Oct.). "Yeni Türkiye sismik tehlike haritasının Ege Bölgesi için değerlendirilmesi." *Niğde Ömer Halisdemir Üniversitesi Mühendislik Bilimleri Dergisi.* 9 (1), pp. 414-423. Available: 10.28948/ngumuh.617268

[26] H., Sucuoğlu. (2019, June). "2019 Türkiye Bina Deprem Yönetmeliğinde başlıca yenilikler." *Turkish Journal of Earthquake Research.* 1(1), pp. 63-75. Available: https://dergipark.org.tr/tr/pub/tdad/issue/46355/567261

[27] SAP2000 (2015) Integrated finite element analysis and design of structures basic analysis reference manual, *Computers and Structures, Inc.* California, USA.

[28] Turkish Standard Institute, TSE. "Requirements for Design and Construction of Reinforced Concrete Structures, TS-500, Ankara. 2000.

[29] N. Caglar. A. Demir. H. Ozturk. and A. Akkaya. (2015, Mar.). "A new approach to determine the moment-curvature relationship of circular reinforced concrete columns." *Computers and Concrete.* 15 (3), pp. 321-335. Available: http://koreascience.or.kr/article/JAKO201509364589469.page

[30] F. Saeid. and S.B. Yuksel. (2020, Jan.) "Investigation of the moment-curvature relationship for reinforced concrete square columns." *Turkish Journal of Engineering.* 4 (1), pp. 36-46. Available: https://dergipark.org.tr/en/pub/tuje/issue/49320/571598

[31] N. Caglar. A. Demir. H. Ozturk. and A. Akkaya. (2015, Nov.). "A simple formulation for effective flexural stiffness of circular reinforced concrete columns." *Engineering Applications of Artificial Intelligence.* 38, pp. 79-87. Available: https://www.sciencedirect.com/science/article/pii/S0952197614002516

[32] Mander J.B., Priestley M.J.N., Park R. (1998, Sep.). "Theoretical stress-strain model for confined concrete." *ASCE Journal of Structural Engineering*. 114 (8), pp. 1804-1826. Available: https://doi.org/10.1061/(ASCE)0733-9445(1988)114:8(1804)

[33] O. Merter, T. Uçar. "Betonarme Çerçevelerin Deprem Hesabında Tasarım İvme Spektrumu Uyumlu Dinamik Yöntemlerin Karşılaştırılması." 3. Türkiye Deprem Mühendisliği ve Sismoloji Konferansı, 2015, pp 1-10.